JOURNAL OF MATERIALS SCIENCE 13 (1978) 1647–1657

Microstructural characterization of cast nickel aluminium bronze

E. A. CULPAN, G. ROSE
Admiralty Underwater Weapons Establishment, Portland, Dorset, UK

The morphology and chemical analysis of the complex phases present in cast nickel aluminium bronze, of nominal composition 10% aluminium, 5% nickel and 5% iron, have been investigated using optical and electron microscopy techniques and energy dispersive analysis. It has been shown that α, β and four forms of κ can exist in the as-cast microstructure of this alloy. Heat treatment can lead to the precipitation of a further κ phase which differs in morphology and chemical composition to those present in as-cast structures.

1. Introduction

Nickel aluminium bronze cast alloy to BS 1400 AB2 is being used increasingly where high strength, high impact properties and good corrosion resistance are required. This alloy, of nominal composition 9.5% aluminium, 5% nickel, 5% iron and copper remainder has replaced the binary aluminium bronze in many applications. Under equilibrium conditions binary alloys, containing up to 9.4% aluminium, form a single phase α solid solution at room temperature, with the strength being directly proportional to the aluminium content. Further addition of aluminium normally results in an $\alpha + \beta$ structure in metal cooled at moderate rates, but decomposition of the β phase will occur during slow cooling or annealing below 565° C to form an $\alpha + \gamma_2$ eutectoid. The presence of this eutectoid decreases both mechanical properties and corrosion performance, therefore steps have to be taken to eliminate the γ_2 phase. One possibility is to heat treat the alloy between 600 and 800° C followed by a rapid air cool or quench which suppresses the β transformation, but unless the cooling rate is sufficiently rapid, the γ_2 phase may still be formed. A further method is to add alloying elements which retard the formation of γ_2 while maintaining the high strength properties that characterize aluminium bronze. The principal alloying elements used for this purpose are iron, nickel and manganese. Both nickel and iron combine with aluminium to form a complex phase, designated κ, which effectively increases the amount of aluminium which may be present in an alloy before the γ_2 phase is encountered. Approximately 1% manganese is usually present in these alloys to aid castability, and to retard the β transformation, and is considered to be equivalent to 0.15% aluminium on the phase diagram.

Because of the complex nature and small volume fraction of many phases present in nickel aluminium bronze, and the non-equilibrium cooling conditions usually encountered, identification and analysis of the phases and the mechanisms by which they are produced have proved difficult to determine. This paper describes an investigation using optical microscopy, scanning electron microscopy (SEM) and scanning transmission electron microscopy (STEM) coupled to an energy dispersive analysis system to characterize the phases present in this alloy system, and to follow the modifications to the structure produced by heat treatment. The amount and distribution of the phases in nickel aluminium bronze and their chemical composition has a significant effect on the properties of this material. The influence of microstructure on fracture behaviour [1] and on corrosion properties [2] are the subject of further publications.

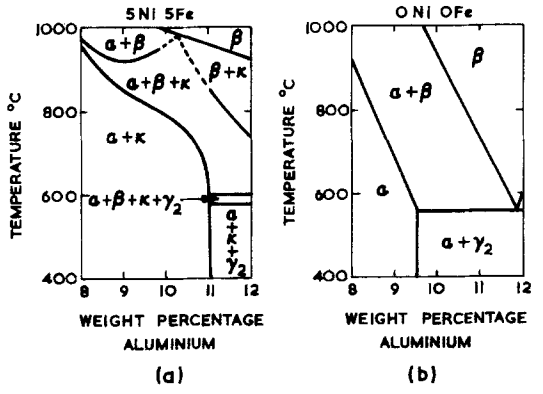

Figure 1 (a) Vertical section of the Cu–Al–Ni–Fe system at 5% Ni, 5% Fe. (b) Binary Cu–Al system.

2. Cast alloy microstructures

The constitution of the copper–aluminium alloys containing 5% nickel, 5% iron from the work of Cook, *et al.* [3], is shown in Fig. 1, together with the binary copper–aluminium diagram for comparison. According to earlier workers [4–6] the alloys complete solidification as a single phase β structure. On further cooling the α phase grows at the β grain boundaries and along crystallographic planes to form a Widmanstätten structure. The nickel–iron–aluminium κ is then precipitated from the β as rounded or dendritic "rosettes" rich in iron, whereas at lower temperatures a lamellar form of κ is produced together with further deposition of α on existing α areas. This continues until all the β has transformed to α and κ, although small areas of retained β can be found in most as-cast structures. Finally there is a precipitation of a fine κ-phase within the α boundaries. This is summarized schematically in Fig. 2.

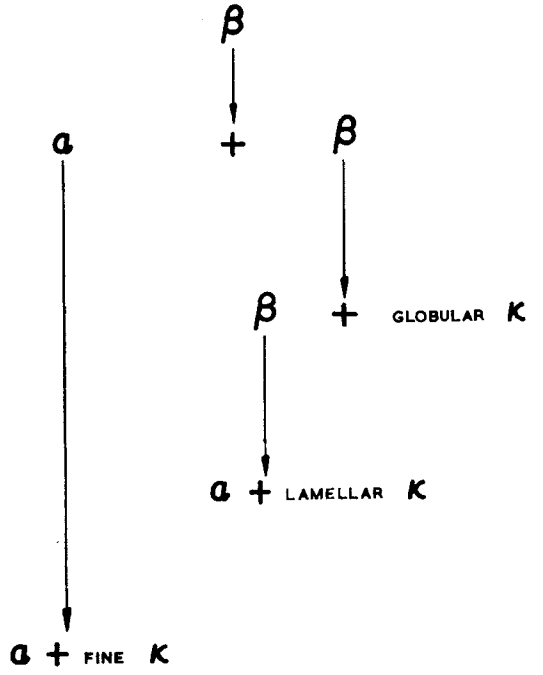

Figure 2 Schematic representation of β phase breakdown.

Work by Weill-Couly and Arnaud [7] has identified various forms of the κ-phase that are evident in cast nickel aluminium bronze, as shown in Fig. 3. Using probe microanalysis they obtained an indication of the chemical composition of some of the phases. These were identified as follows:

κ_I a rosette form of composition 6% Al, 8% Ni, 69% Fe, 13% Cu.

κ_{II} and κ_{III} a globular or lamellar form of composition 18 to 20% Al, 23 to 34% Ni, 26 to 43% Fe, 13 to 20% Cu.

κ_{IV} a fine precipitate within the α grains, thought to be iron-rich.

More recently Duma [8] investigated the structure and analysis of the κ phases, and identified the κ phases according to their morphologies. The analyses of the respective phases are shown in Table I, together with the identification adopted by Weill-Couly and Arnaud. Duma [8] did not isolate the κ_{III} and κ_{IV} during analysis and the results quoted include the surrounding α matrix. In fact the analyses for $\kappa_{III} + \alpha$ and $\kappa_{IV} + \alpha$ are not very different from that of the α matrix, indicating a low volume fraction of precipitate within the electron beam.

3. Development of microstructure

Specimens used in this investigation were held at 1000° C for 1 h and subsequently cooled to successively lower temperatures at 25° C intervals, at a rate of 8° C min^{-1}, to simulate cooling of 25 mm castings, before quenching in cold water. Under these conditions the phase transformations

TABLE I

Phase	Compositon (wt %)			
	Cu	Al	Ni	Fe
Large globular phase (κ_I)	9	14	6.5	64
Lamellar two-phase eutectoid ($\kappa_{III} + \alpha$)	82	9	3	3
Fine two-phase intermixture ($\kappa_{IV} + \alpha$)	83	9	3	4
α matrix	87	6.5	7.5	3

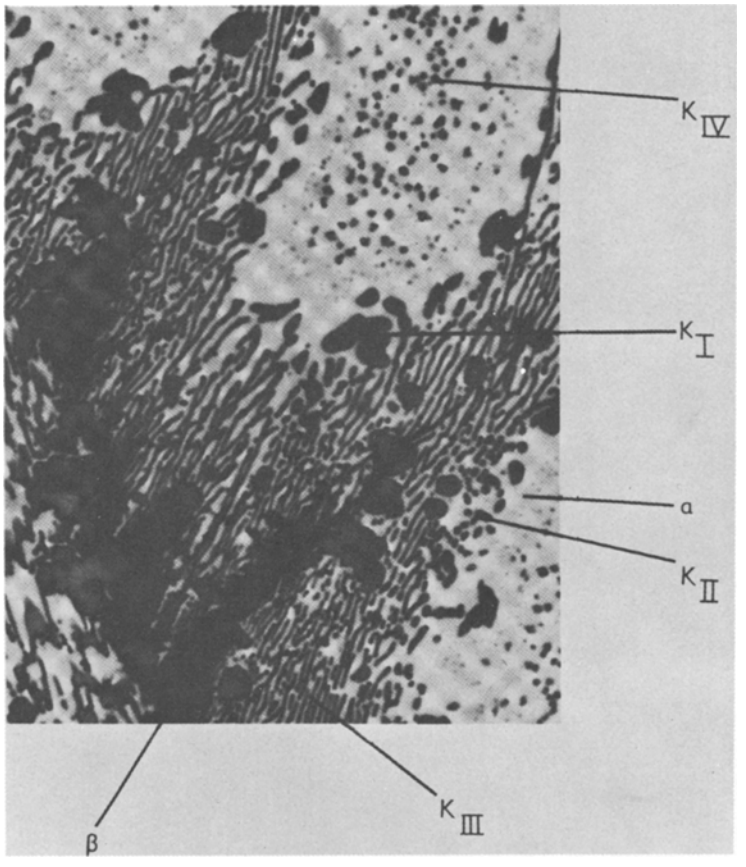

Figure 3 Microstructure of sand cast nickel aluminium bronze showing constituent phases (× 750).

occurred as shown in Table II. Although non-equilibrium cooling depresses the phase transformation temperatures it is interesting to note that the room temperature volume fractions of the various phases approach those predicted from the equilibrium diagram (Fig. 1).

Figs. 4 to 6 indicate the phase changes of nickel aluminium bronze at various temperatures. After quenching from 1000° C the alloy is wholly β phase, however on cooling to 900° C (Fig. 4) areas of light etching α are formed. The grey etching rosette κ phase precipitates randomly in the α and β phases, although traditionally thought to be formed only from the β. The breakdown of the β phase is seen to take place at the α/β boundaries – the lamellar phase grows at right angles to this α/β boundary. It is possible that the lamellar κ_{III} and globular κ_{II} are essentially similar in chemical composition as they are being rejected at the same temperature from the same phase. The similarity of the κ_{II} and κ_{III} phases can be seen from Fig. 5 which illustrates κ_{II} and κ_{III} growing together. It is probable that the rosette κ_I phase can nucleate the κ_{III} around its perimeter, which may explain the dark etching band surrounding κ_I particles shown in as-cast microstructures. This is shown more clearly in Fig. 6 where the continuity between the lamellar form of κ_{III} and the surrounding band is evident. At temperatures slightly below the $\beta \rightarrow \alpha + \kappa_{II} + \kappa_{III}$ transformation, precipitates of κ_{IV} are noted within the grains (Fig. 7).

TABLE II

Phase transformation	Equilibrium transformation temperature (° C)	"25 mm casting" transformation temperature (° C)
$\beta \rightarrow \alpha + \beta$	1010	925
$\beta \rightarrow \alpha + \kappa_I$	900–920	820–830
$\beta \rightarrow \alpha + \kappa_{II} + \kappa_{III}$	840–870	775–750
$\alpha \rightarrow \alpha + \kappa_{IV}$	–	700–675

An electrolytically etched surface of an as-cast microstructure (Fig. 8) shows clearly the lamellar structure of the κ_{III} phase.

The crystal structures of the phases described above are not well characterized. Recent electron diffraction studies of the α phase by the authors have confirmed a f c c structure with $a = 3.57$ Å.

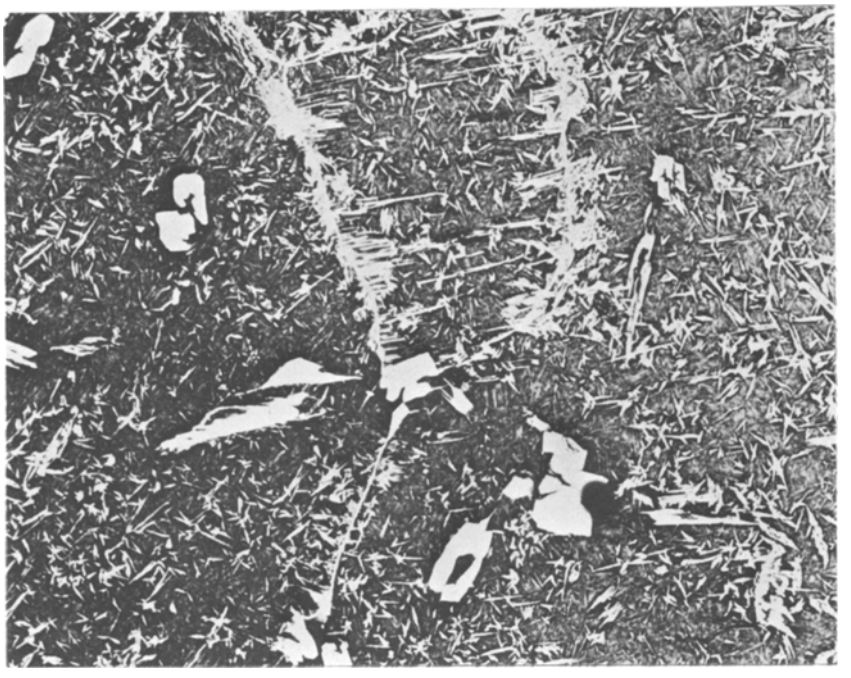

Figure 4 Alloy slowly cooled from 1000 to 900° C and quenched, showing nucleation of α phase (× 100).

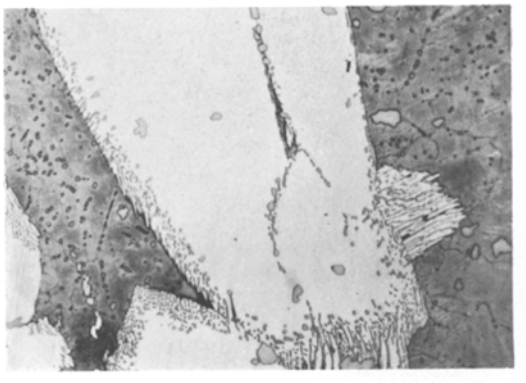

Figure 5 Alloy slowly cooled from 1000 to 800° C and quenched, showing formation of κ_{II} and κ_{III} at the α/β interface (× 480).

Figure 7 Alloy slowly cooled from 1000 to 725° C and quenched, showing fine κ_{IV} precipitation within the α grains (× 480).

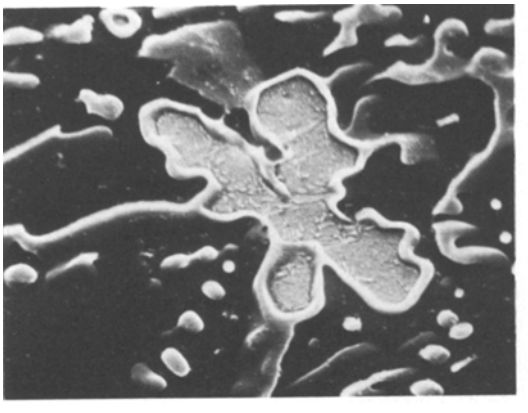

Figure 6 Rosette κ_I surrounded by lamellar κ_{III} phase (× 6500).

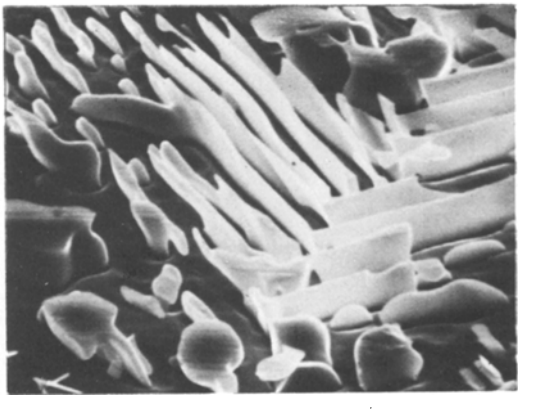

Figure 8 Lamellar κ_{III} phase (× 6500).

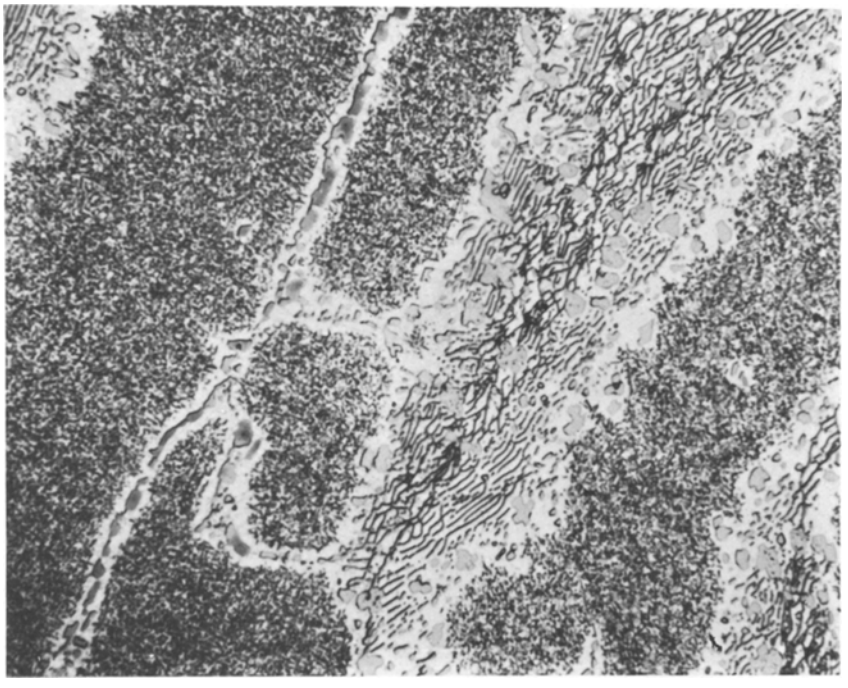

Figure 9 Alloy heat treated at 675° C for 6 h (× 600).

This compares favourably with α in Cu–10% Al with $a = 3.62$ Å. The crystal structure of the high temperature β phase cannot be confirmed by normal electron diffraction techniques, as a complex martensitic structure is obtained on quenching from the β phase field. The normal high temperature β phase cannot exist at room temperature and the, so-called, "retained β" should be described as β'. The structure of the martensite has been described as distorted hcp [9] and recently as a mixture of fcc and hcp [10].

Recent neutron diffraction [11] studies have confirmed that the rosette κ_I has a body centred cubic (b2) type of structure with a lattice parameter of 2.97 Å. No crystal structure determinations of the lamellar and globular phases in nickel aluminium bronze have been reported.

4. Heat treatment of nickel aluminium bronze

Heat treatment of the as-cast nickel aluminium bronze at temperatures under 840° C did not produce any changes in the major phases present except that retained β' was transformed to $\alpha + \kappa$. There was however a significant increase in the amount of fine precipitate present within the α grains, shown in Fig. 9. Closer examination of these precipitates has shown that the precipitates were a mixture of two distinct forms. One type, usually spheroidal (approximately 1 μm in diameter) but on occasions closely resembling tiny κ_I rosettes, was iron-rich, and was probably connected with the κ_{IV} precipitation within the α grains found in as-cast materials. The second form (approximately 1 μm × 0.1 μm) designated by the authors as κ_V was cylindrical or lath-shaped and was rich in nickel and aluminium. The exact analyses of these phases are discussed in a later section.

Increasing the heat treatment temperature resulted in an increase in the size of the lath κ_V precipitates and the apparent disappearance of the globular κ_{IV} phase. This trend continued until at 840° C (Fig. 10), the κ_V phase having increased

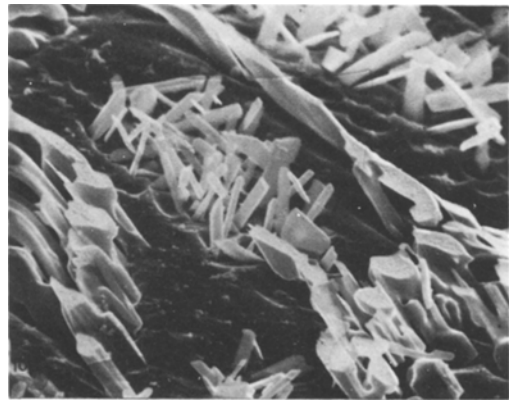

Figure 10 Alloy heat treated at 840° C for 3 h (× 3250).

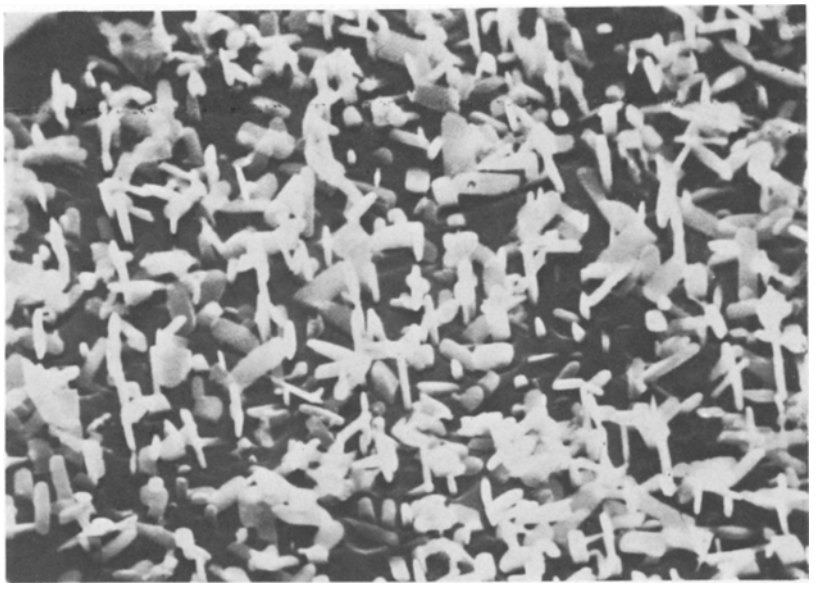

Figure 11 Alloy heat treated at 675° C for 16 h (× 10 000).

in size to a large rod-like form (approximately 10 μm × 2 μm). A similar trend was noticed when the alloys were held for longer times at lower temperatures, although the precipitate sizes were significantly smaller (~ 1 μm × 0.5 μm) (Fig. 11).

At treatment temperatures above 820 to 850° C the alloy can enter the $\beta + \alpha + \kappa$ region depending on its exact composition. Heat treatment in this region for sufficient time resulted in spheroidization of the κ phase and the resulting structure is shown in Fig. 12.

There are various additional heat treatments that could be carried out on nickel aluminium bronze, in particular by quenching from elevated temperatures and tempering in an analogous manner to steel heat treatment. However these treatments are rarely applicable to large castings and have not been included in this paper.

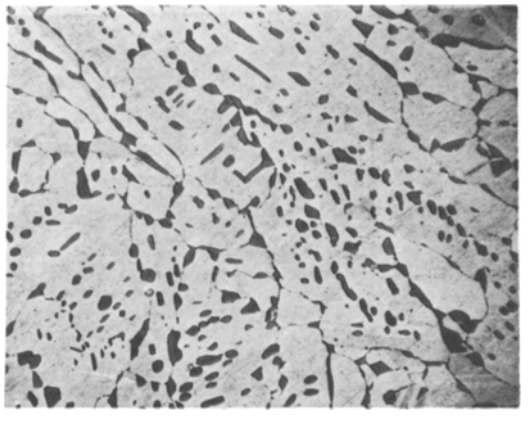

Figure 12 Alloy heat reated at 860° C for 72 h (× 480).

5. Chemical analysis of constituent phases

5.1. Experimental

5.1.1. Bulk specimens

As-cast specimens for phase analysis were held at 1000° C (i.e. in the β phase field) for 1 h and then cooled at 8° C min^{-1} to intermediate temperatures before quenching in cold (20° C) water. The intermediate temperatures were 975° C reducing by 25° C intervals to 675° C.

Phase analysis was also carried out on heat treated specimens. The heat treatments employed were:

(a) 675° C – 2 h, 6 h and 16 h air-cooled;
(b) 740° C 3 h air-cooled;
(c) 790° C 3 h air-cooled;
(d) 840° C 3 h air-cooled;
(e) 860° C 72 h air-cooled.

Both as-cast and heat treated specimens were prepared for analysis by normal metallographic techniques. The specimens were examined on a Cambridge Scientific Instruments S600 SEM with a Link Systems Energy Dispersive Analysis attachment. Analyses were carried out with a spot size of 200 Å and the data computed using the Nazir technique [12].

Two stage carbon replicas were also taken from etched specimens and the extracted phases analysed in the STEM mode on a JEOL 100B electron microscope with an Energy Dispersive attachment.

5.1.2. Thin foil specimens

3 mm diameter electron transmission thin foil specimens in the as-cast condition were prepared

by ion beam machining and examined using a JEOL 100B/ASID electron microscope with a Link Systems Energy Dispersive Analysis attachment in the STEM mode. A spot size of about 200 Å in diameter was used for analysis.

The chemical composition of both bulk and thin foil specimens was as follows: Al 9.42%; Ni 4.70%; Fe 4.24%; Mn 1.09%; copper remainder.

5.2. Analysis techniques

5.2.1. Bulk specimens

The quantitative analysis of bulk specimens by solid state Si(Li) X-ray detectors on scanning electron microscopes has developed rapidly over the last few years. The technique requires comparison of the characteristic X-ray peak intensity (I_x) in the unknown sample with that of a well-defined standard (e.g. pure X). Numerous computer programs are available to evaluate the required atomic number (Z), absorption (A) and secondary fluorescence (F) corrections to the data obtained (ZAF). The accumulation of data from a multi-component alloy takes a considerable time and difficulty has been experienced in maintaining instrumental parameters constant during analysis. This has been found to be a significant source of error.

To reduce the analysis time Nazir [12] has deduced analytical expressions and computed normalization factors which compensate for atomic number corrections and X-ray transmission through the solid state detector. These factors allow concentrations to be calculated directly from the peak intensities of the alloy examined, without reference to standards.

In the analysis of nickel aluminium bronze the predominant correction is the absorption correction with respect to aluminium. To eliminate the necessity for computer correction, empirical absorption correction factors for aluminium in copper have been evaluated by analysing a series of Al–Cu alloys using a ZAF correction program and comparing the results with the data from the standardless technique of Nazir. The difference in the two sets of results represents, to a first approximation, the degree of absorption correction for aluminium in copper. The fluorescence correction is minimal. This technique has shown itself to have an accuracy comparable with the ZAF correction computer program with a significant decrease in analysis time [13].

5.2.2. Thin foils

The technique employed was essentially that of Cliff and Lorimer [14] whereby quantitative analysis was obtained from a thin foil specimen with the X-ray intensities of the two elements measured simultaneously (at a constant kV and independent of specimen thickness). Thus

$$\frac{C_1}{C_2} = \frac{k_1 I_1}{k_1 I_2}$$

where C_1 and C_2 are the concentrations of two elements in alloy (wt%), k_1 and k_2 are intensity correction factors for the two elements, and I_1 and I_2 are characteristic X-ray intensities for each element.

The correction factors for the elements were evaluated by analysing standards of known chemical composition and the resulting factors are shown in Table III for analysis at 100 kV.

6. Results

The average chemical analysis of the six phases usually found in as-cast nickel aluminium bronze, using SEM and STEM (both thin foil and replicas) are shown in Table IV.

In most cases between 20 and 30 analyses were taken of each phase present and the standard deviations of these results are also shown in Table IV. No standard deviations are quoted when the number of analyses taken were less than 10. It is apparent from the analysis results that the chemical composition of constituent phases in nickel aluminium bronze can vary quite appreciably from specimen to specimen and within the same specimen. This is particularly pronounced with the various κ phases, indicating that they can exist over a wide range of chemical composition. The globular κ_I and κ_{IV} phases have similar compositions rich in iron, and are thought to be Fe_3^*Al

TABLE III Calibration factors (k) for JEOL 100B/STEM at 100 kV

Element	Factor (k)
Mg	2.858
Al	1.711
Si	1.000
Ca	1.106
Mn	1.118
Fe	1.196
Ni	1.410
Cu	1.548
Zn	1.655

TABLE IV Chemical analysis of phases present in cast nickel aluminium bronze

Phase	SEM/bulk					STEM/thin foil					STEM/replica				
	Al	Mn	Fe	Ni	Cu	Al	Mn	Fe	Ni	Cu	Al	Mn	Fe	Ni	Cu
α	8.3 ± 1.7	1.4 ± 0.1	2.7 ± 2	2.5 ± 1.4	85.4 ± 4	8 ± 2	0.8 ± 0.3	2.4 ± 1	3 ± 2	86 ± 4	–	–	–	–	–
β	8.7	1.0	1.6	3.5	85.2	–	–	–	–	–	–	–	–	–	–
κ_I	13 ± 5	2 ± 0.4	55 ± 7	15 ± 3	15 ± 5	–	–	–	–	–	–	–	–	–	–
κ_{II}	19 ± 3	2.2 ± 0.6	32 ± 3	27 ± 4	21 ± 5	18 ± 4	1.6 ± 0.3	34 ± 5	24 ± 5	23 ± 4	19 ± 5	1.3 ± 0.1	34 ± 5	30 ± 3	15 ± 5
κ_{III}	18 ± 6	2 ± 0.3	22 ± 0.7	32 ± 2	26 ± 4	22 ± 4	1.6 ± 0.4	22 ± 5	28 ± 5	26 ± 4	–	–	–	–	–
κ_{IV}	20 ± 3	1.5 ± 0.3	62 ± 4	4 ± 1	13 ± 1	9 ± 4	1.6 ± 0.4	60 ± 8	6 ± 4	23 ± 6	14 ± 2	1.1 ± 0.4	63 ± 6	14 ± 4	8 ± 3

where Fe* is iron plus minor additions of copper, nickel and manganese. The κ_{II} and κ_{III} also have a wide range of compositions, and there appears to be a significant difference in the nickel:iron ratio of these phases which is consistent for each analysis technique. In the case of κ_{II} the percentage of iron generally exceeds that of nickel by approximately 5 to 10%, whereas in κ_{III} nickel exceeds iron by a similar amount. It is apparent therefore that there are statistically significant differences in the composition of κ_{II} and κ_{III} despite the fact that these phases are precipitated from the matrix at the same temperature.

Analyses were also carried out on the boundary layer surrounding the κ_I phase, typically shown in Fig. 7, and the mean analysis of this layer was: Al 16%; Mn 1.2%; Fe 22%; Ni 34%; Cu 26%. This is consistent with a κ_{III} analysis indicating a deposition of lamellar κ on the rosette κ_I phase.

The composition of the retained β phase in specimens that had been quenched from decreasing temperatures from 975 to 675° C is shown in Fig. 13. Only the major elements iron, nickel and aluminium are displayed, as it is clear from the previous work that manganese is distributed evenly throughout the material. It can be

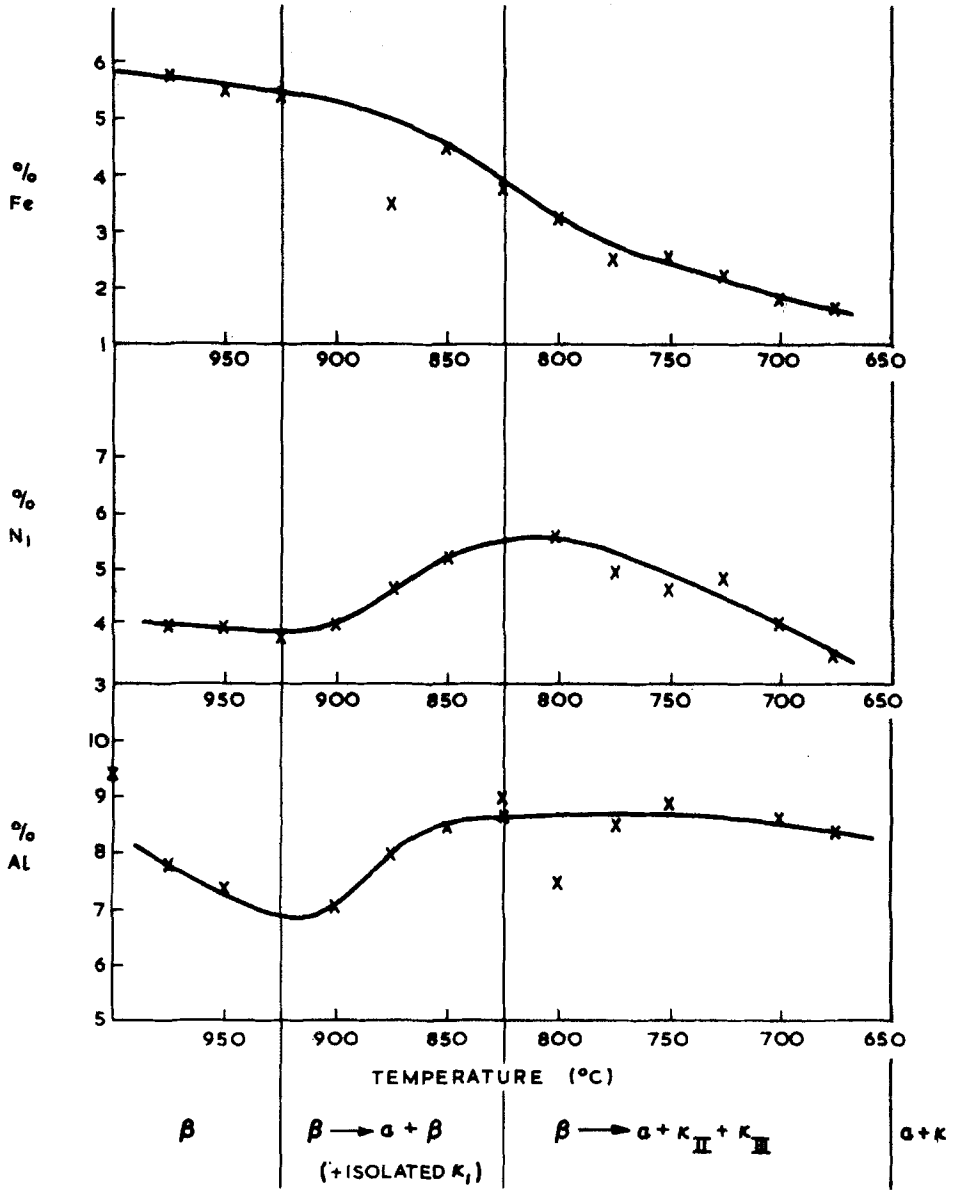

Figure 13 Variation of β composition with respect to temperature.

seen in Fig. 13 that the composition of the β accurately reflects the changes caused by the transformation to α and κ phases. Below 900° C the large iron rich κ_I rosettes are formed with a corresponding decrease in the iron content of the β. This results in a slight increase in the aluminium and nickel content of the β until 825° C, where the κ_{II} and κ_{III} (Ni Al–Fe Al) phases start to form, with a consequent decrease in aluminium, nickel and iron in the β.

A similar survey of the changes in composition of α from its formation around 900° C down to room temperature was carried out. Little change in α composition was noted through the temperature range with the exception of iron content which was approximately 5% at 900° C and was reduced to 2.7% at room temperature. This is consistent with formation of an iron-rich precipitate within the α phase on cooling.

The analyses carried out on the fine precipitates within the α grains following various heat treatments are shown in Table V. These results confirm the microscopical evidence that the high iron κ_{IV} phase is not apparent following heat treatments at temperatures greater than 740° C or at 675° C for 16 h. The lath-like κ_V precipitate, found in increasing volume as the heat treatment temperature is raised, contains a substantial amount of aluminium, nickel and iron. It is interesting that the proportion of iron found in the phase increases as the temperature of heat treatment is raised, indicating that the iron-rich κ_{IV} phase is taken up by the κ_V phase. This high temperature κ_V has a composition similar to that of the annealed κ produced after heat treatment at 860° C for 72 h. Thus it is possible that an equilibrium κ phase is produced locally in the α grains under the influence of heat treatment. Equilibrium conditions are more likely to develop in this area than elsewhere due to very large surface area to volume of these particles and their extremely close proximity to each other as shown in Fig. 11. Under these conditions diffusion should be enhanced even at moderate heat treatment temperatures.

7. Conclusions

(1) Optical and electron microscopy techniques have been successful in identifying and analysing the microstructural phases in cast nickel aluminium bronze, namely α, β and four κ phases.

(2) The microstructural changes that occur during heat treatment lead to the precipitation of a further κ phase which differs in morphology and chemical composition to those present in as-cast structures.

Acknowledgements

The authors wish to thank Mrs A. E. Morris, Mr K. Stokes and Mr D. Moth for their assistance during this investigation. Any views expressed are those of the authors and do not necessarily represent those of the Procurement Executive, Ministry of Defence. This paper is printed with the kind permission of the Controller, HMSO, holder of Crown Copyright.

References

1. E. A. CULPAN and J. T. BARNBY, *J. Mater. Sci.* **13** (1978) 323.
2. E. A. CULPAN and G. ROSE (to be published).
3. M. COOK, W. P. FENTIMAN and E. DAVIES, *J. Inst. Met.* **80** (1951) 419.
4. W. L. J. CROFTS, D. W. TOWNSEND and A. P. BATES, *British Foundryman* **57** (1964) 89.
5. P. J. MACKEN and A. A. SMITH, "The Aluminium Bronzes", Copper Development Association Publication No. 31 (1966).

TABLE V Chemical analysis of the fine precipitates within the κ phase of heat treated nickel aluminium bronze

Phase	SEM/bulk					STEM/replica				
	Al	Mn	Fe	Ni	Cu	Al	Mn	Fe	Ni	Cu
κ_{IV} globular phase (675° C for 2 h)						13 ± 3	1 ± 0.2	62 ± 6	16 ± 3	8 ± 3
κ_V lath phase (675° C for 2 h)						23 ± 2	1 ± 0.3	25 ± 3	39 ± 2	11 ± 1
κ_{IV} globular phase (675° C for 6 h)						14 ± 2	1 ± 0.5	63 ± 6	14 ± 5	8 ± 5
κ_V lath phase (675° C for 6 h)						27 ± 4	1.5 ± 0.3	27 ± 4	35 ± 3	10 ± 2
κ_V lath phase (675° C for 16 h)						20 ± 3	1.3 ± 0.3	34 ± 3	35 ± 2	10 ± 1
κ_V lath phase 740° C	26	1.1	26	21	26	21 ± 2	1.8 ± 0.5	33 ± 3	35 ± 2	9 ± 2
κ_V lath phase 790° C	23	1.2	33	21	22	18 ± 2	1.6 ± 0.3	40 ± 2	30 ± 1	10 ± 1
κ_V large lath phase 840° C	25	1.1	34	21	19	17 ± 3	1.7 ± 0.1	39 ± 5	32 ± 3	10 ± 1
Spheroidized κ phase (840° C for 3 days)	19	1.6	35	24	21	17 ± 2	1.6 ± 0.2	40 ± 3	31 ± 3	10 ± 1

6. J. N. BRADLEY, unpublished work (1967).
7. P. WEILL-COULY and D. ARNAUD, *Fonderie* **28** (1973) 123.
8. J. A. DUMA, *Naval Eng. J.* **87** (1975) 45.
9. W. B. PEARSON, "Handbook of Lattice Spacings and Structures of Metals and Alloys" (Pergamon, Oxford, 1964) p. 331.
10. J. J. REGIDOR, M. A. CRISTINA and J. M. SISTIAGA, *Rev. Metal. Cenim* **10** (1974) 165.
11. J. G. BOOTH, private communication (1977).
12. M. NAZIR, *J. Microscopy* **108** (1976) 79.
13. G. ROSE and D. A. MOTH, private communication (1977).
14. G. CLIFF and G. W. LORIMER, Proceedings of the Fifth European Congress on Electron Microscopy, Manchester (Institute of Physics, London, 1972).

Received 30 August and accepted 14 November 1977.